Published in final edited form as:
J Org Chem. 2007 December 7; 72(25): 9722–9731. doi:10.1021/jo7017922.

Studies on A Urea Directed Stork-Crabtree Hydrogenation. Synthesis of C1–C9 Subunit of (+)-Zincophorin

Zhenlei Song, **Richard P. Hsung***, **Ting Lu**, and **Andrew G. Lohse**
Division of Pharmaceutical Sciences and Department of Chemistry, Rennebohm Hall, 777 Highland Avenue, University of Wisconsin, Madison, WI 53705

Abstract

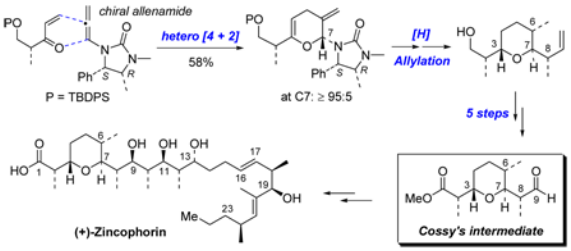

A detailed account on the stereoselective synthesis of the C1–C9 subunit of (+)-zincophorin is described here. This approach features the first application of a stereoselective inverse electron demand hetero [4 + 2] cycloaddition of chiral allenamides in natural product synthesis. The C1–C9 subunit matches Cossy's intermediate, thereby constituting a formal total synthesis. In addition, details of an unusual urea directed Stork-Crabtree hydrogenation observed during these efforts is also disclosed here.

INTRODUCTION

Polyoxygenated ionophore-containing natural products exhibit potent anti-infectious properties through proton-cation exchange processes across biological membranes. This activity is due to the ability of ionophores to form lipophilic complexes with various cations such as Li^+, Na^+, and K^+, and divalent alkaline earth cations such as Ca^{2+} and Mg^{2+}.[1] In 1984, two new monocarboxylic acid ionophores, griseocholin and antibiotic M144255, were isolated from cultured strains of *Streptomyces griseus*.[2] Extensive NMR experiments of griseocholin and X-ray diffraction of the zinc-magnesium salt of M144255 revealed that these two compounds are actually structurally identical with the same absolute configuration.[2b] Based on its ability to strongly bind with Zn^{2+}, it was given the trivial name (+)-zincophorin (Figure 1). (+)-Zincophorin possesses strong *in vivo* activity against Gram-positive bacteria and *Clostridium coelchii*. Its ammonium and sodium salts display significant anti-coccidal activity against *Eimeria tenella* in chicken embryos, and its methyl ester was reported in a patent as having strong inhibitory properties against influenza WSN/virus with reduced toxicity for the host cells.[2d, 3]

Over the last twenty plus years, (+)-zincophorin has attracted an impressive array of synthetic efforts including Danishefsky's first total synthesis along with two recent elegant total syntheses reported by Cossy and Miyashita.[4] We recently communicated our formal total

rhsung@wisc.edu.

syntheses of (+)-zincophorin via interception of Miyashita's advanced intermediate.[5] The key strategy features our previously reported stereoselective inverse electron demand hetero-[4 + 2] cycloaddition of chiral allenamides (Scheme 1).[6–9] Herein, we report the synthesis of Cossy's C1–C9 subunit of (+)-zincophorin based on this approach, as well as details of the observation of an unusual urea directed Stork-Crabtree hydrogenation.

RESULTS AND DISCUSSIONS

1. Retrosynthetic Plan

The construction of Cossy's intermediate **6**, or the C1–C9 subunit of (+)-zincophorin, could be realized from tetrahydropyran **7**, which contains all prerequisite stereocenters by several transformations (Scheme 2). In turn, tetrahydropyran **7** could be prepared from pyran **8** via: 1) stereoselective hydrogenation of *exo*- and *endo*-cyclic olefins from less hindered top face of the pyranyl ring; and 2) a Lewis acid promoted stereoselective crotylation to remove imidazolidinone auxiliary.[10] Finally, the inverse electron demand hetero-[4 + 2] cycloaddition of chiral allenamide **9** with enone **10** could establish the pyranyl skeleton in **8**.

2. Synthesis of Chiral Allenamide 9 and Enone 16

Synthesis of chiral allenamide **9** commenced from (+)-ephedrine hydrochloride salt **11** and urea. By condensation of the mixture at 175°C for 0.5 h and then 200–210 °C for 1.5 h, the so-called Close auxiliary **12** could be obtained in 48% yield after recrystallization.[11] Subsequently, propargylation followed by base-catalyzed isomerization of propargyl amide **13** furnished chiral allenamide **9** in 93% overall yield (Scheme 3). In the same manner, with the enantiomer of ephedrine, allenamide *ent*-**9** was also prepared.

Chiral enone **16** was prepared from the commercially available chiral hydroxy ester **14** as shown in Scheme 4. Protection of the hydroxyl group as a TBDPS ether followed by reduction of the ester group using DIBALH afforded aldehyde **15** in 76% overall yield.[12] Subsequent vinyl Grignard addition and Swern oxidation of the resulting isomeric mixture (1:1) of allylic alcohols gave rise to chiral enone **16** with an overall yield of 66%.

3. Inverse Demand Hetero-[4 + 2] Cycloaddition

With chiral allenamides **9** and *ent*-**9**, in hand, we pursued the key inverse demand hetero-[4 + 2] cycloaddition. Concerned with the fact that the stereochemical outcome could be controlled either through the chiral auxiliary of the allenamide or the chiral enone, leading potentially to matched and/or mismatched scenarios, we examined both reactions of chiral allenamides **9** and *ent*-**9** with enone **16** (Scheme 5). By using our reported cycloaddition protocol with CH_3CN as the solvent and the sealed tube as the reaction vessel, after heating at 85°C for 48 h, both reactions of **9** and *ent*-**9** with **16** proceeded readily to provide pyrans **17** and **18** in 58% and 54% yield, respectively, as single isomers. The stereochemistry of **18** was unambiguously confirmed by its single-crystal X-ray diffraction analysis.

Given that the reaction of chiral allenamide **9** should proceed through the matched transition state model shown in Scheme 5 [on the right side], the stereochemical assignment for **18** and the high level of selectivity imply that the cycloaddition of *ent*-**9** also proceeded through the related transition Scheme 5 state, although potentially mismatched [on the left side]. However, any mismatching perceived or real clearly did not impede the reaction or the stereoselectivity. A closer examination reveals that to allow the chiral enone to still approach the open π-face of the internal olefin of allenamide *ent*-**9** as dictated by the chiral Close auxiliary, and to avoid any mismatching as well as allylic strain, the heterodiene **16** would need to position the Me group on the alpha carbon orthogonal to the plane of the chiral enone (Scheme 5).

4. Hydrogenations of Pyran 17 and A Urea Directed Stork-Crabtree Hydrogenation

(a) Hydrogenation of the C6 Exo-Cyclic Olefin—Our efforts then encountered a serious obstacle at what we had believed to be the most trivial stage: sequential hydrogenations of the two olefins at C6 and C3. Given that the *exo*-cyclic olefin at C6 is more accessible sterically, we intended to accomplish this hydrogenation via mild conditions to ensure good stereoselectivity. As shown in Scheme 6, Lindlar catalyst in MeOH was initially deployed (entry 1), but after stirring for 2 d at 1 atm H_2, the desired mono-hydrogenation product **19** was obtained with a best yield of 44% while being contaminated with 23% of the ring-opened byproduct ketone **20** as a 3:2 isomeric mixture with regards to C6. Although increasing the H_2 pressure to 60 *psi* did shorten the reaction time (entry 2), the yield dropped drastically while providing a large amount of ketone **20**.

We initially believed that the formation of ketone **20** was initiated via hydrolysis of the cyclic aminal through protonation of the electron rich C3 *endo*-cyclic olefin. Given this consideration, EtOAc and anhydrous hexanes (entries 3 and 4) were employed as solvents, but the formation of **20** still persisted. Changing metal catalyst from Pd to Pt appeared not to be useful either (entry 5). However, intriguingly, we found that without H_2, pyran **17** was actually quite stable in the presence of Pt/C catalyst in MeOH (entry 6).

These observations led us to speculate that the formation of ketone **20** is likely promoted by the catalyst-activated H_2. As shown in Scheme 7, the same Pt-complex **21** from pyran **17** that could lead to the desired mono-hydrogenation product **19** could also protonate the electron rich *endo*-cyclic double bond as shown in Pt-complex **22**. This would result in ring-opening to give the Pt-π-allyl type complex **23**, leading to alkene **24** after reductive elimination. Further hydrogenation of **24** should give **20** as an isomeric mixture as observed. Alternatively, the mono-hydrogenation of pyran **17** could take place predominantly to exclusively afford dihydropyran **19** initially, but **19** could be subsequently converted into **20** via complex **25** through an analogous sequence.

Given this proposed process, it seemed that identifying a catalyst with appropriative activity that is effective to hydrogenate the *exo*-cyclic olefin but slow to protonate is very important. Ultimately, by screening several kinds of base-poisoned catalysts, we were delighted to find that the hydrogenation of this *exo*-cyclic olefin could be achieved in 64% yield with only 12% of **20** by using Adam's catalyst along with 3.0 equiv of $NaBH_4$ (entry 8 in Scheme 6).

(b) Hydrogenation of the C3 Endo-Cyclic Olefin—Further hydrogenation of the C3 *endo*-cyclic olefin, which is more electron rich and sterically less accessible, turned out to be much more difficult by using any heterogeneous catalysts under 15–70 *psi* of H_2. The formation of the ring-opening product **20** was observed as the major product in most cases with no desired product found (Scheme 8).

However, by using Stork-Crabtree's conditions,[13] the C3 *endo*-cyclic olefin was reduced smoothly and provided presumably the desired tetrahydropyran **26** in 74% yield. Unsuspectingly, we proceeded to remove the silyl group in **26**, only to be confronted with a product quite different as established by the X-ray structure of **27**. While the stereochemistry at C6 is as expected, both stereocenters at C3 and C7 are opposite from what we had expected. These expectations were based on our earlier analyses in which the mono-hydrogenated pyran would assume a unique conformation as shown for **19** (Scheme 8). Hydrogenations of C3 olefin should show a distinct preference at the top face of a flat pyranyl ring away from the urea group, which shields the bottom face while being pseudo-axially situated.

(c) A Urea Directed Stork-Crabtree Hydrogenation.[14–16]—This unexpected outcome implies a number of possibilities. We considered the following two possibilities as

illustrated in Scheme 9. First, the mono-hydrogenation product **19** could epimerize at C7 to give **28** in which the hydrogenation could occur at the bottom face, leading to **27** after desilylation (**pathway-a**). While this pathway is very likely and provides a sound rationale, we suspected a second scenario involving a urea-directed Stork-Crabtree hydrogenation as shown in **29** to give tetrahydropyran **30** prior to a C7-epimerization that would afford **31** (**pathway-b**). Tetrahydropyran **30** differs from **27** only in the protection of the primary OH group.

Toward this end, we carried out the reaction using 2.0 equiv of Na_2CO_3 to scavenge protic species or decrease the Lewis acidity of Ir(I) that could promote the C7-epimerization, and found 11% of **30** (a 1:2 inseparable mixture with **19**) along with 35% of **31**. The relative stereochemistry in **30** was assigned based on the *J* value between H6 and H7 being in the *equatorial-axial* range (Scheme 10). Treatment of the mixture of **30** and **19** in CH_2Cl_2 with a trace amount of *p*-TsOH quickly give **31** via epimerization at C7 in about 60–70% yield. Meanwhile, the relative stereochemistry in **31** was confirmed via silylation of **27** (Scheme 9). These results collectively imply that the hydrogenation at the hindered bottom face of **19** is possible under the Stork-Crabtree conditions.

While **pathway-b** is supported via the above experiment, we still could not rule out **pathway-a** by now. Thus, the following reaction to make dihydropyran **28** was examined. When subjecting **19** to pre-activated Crabtree's catalyst in CH_2Cl_2, **19** was transformed to **28** in 40% yield via epimerization. The relative stereochemistry in **28** was assigned by the *J* value between H6 and H7 being in the *axial-axial* range (Scheme 10). However, under the same directed hydrogenation conditions, dihydropyran **28** could not be converted into **31** and only the ring-opening by-product **20** was formed in about 40% yield.

Based on this result, **pathway-a** in Scheme 9 can be excluded completely. Semi-empirical calculations on pyranyls **19** and **28** were also performed using the Spartan'02 program (Figure 2). Based on the calculation results, **19** seems thermodynamically more favorable than **28**. This is also supported by the acid-catalyzed epimerization experiment in which 2:1 ratio of **19:28** was formed after stirring with PTS in CH_2Cl_2 for 5 h. The molecular models distinctly reveal that in pyran **19**, the urea group occupies the pseudo-axial position allowing the directed hydrogenation to occur, while in pyran **28**, the urea group assumes the pseudo-equatorial position, thereby preventing the coordinated metal center to reach the C3 *endo*-cyclic olefin and thwarting the directed hydrogenation.

(d) Directed Hydrogenation versus C7-Epimerization—Our efforts also led to another observation involving competition between directed hydrogenation and epimerization at C7. As shown in Scheme 11, it appeared that this competition is dependent upon the pressure of H_2, as higher pressure tends to favor the directed hydrogenation product **31**. A potential mechanism was proposed as shown in Scheme 12. Upon treatment with H_2, the unsaturated Crabtree's catalyst could complex to the urea group and to the C3 *endo*-cyclic olefin, leading to the common Ir-complex **32** in which **pathway-c** and **pathway-d** could take place depending upon the pressure of H_2.

Under higher pressure (≥60 *psi*), oxidative addition of H_2 could occur to provide **33** en route to alkyl metal complex **34** via migratory insertion. Reductive elimination and epimerization would yield tetrahydropyran **31** and regenerates the active catalyst. However, with lower pressure (≤60 *psi*), the complexation of H_2 to the Ir metal and the subsequent oxidative addition would be slower, thereby allowing **32** to undergo ring-opening by cleavage of C7-O bond and form the Ir-oxo-π-allyl complex **35**. An ensuing C6–C7 bond rotation could take place to alleviate steric interactions, leading to the more favored conformer **36**, which can afford **28** via ring-closing and release of the Ir-catalyst.

To further explore this urea-direct hydrogenation, we employed the model pyran **37** with the (*R*)-Close auxiliary because we had unambiguously established the stereochemical outcome of its hydrogenations (Scheme 13).[6,10c] Specifically, the mono-hydrogenated product **38** obtained from standard hydrogenations contains exclusively a *cis* relationship for Ha and Hb with a small *J* value. When hydrogenating pyran **37** with the Crabtree's catalyst, we isolated **39** with a large *J* constant, distinctly suggesting a *trans* relationship between Ha and Hb. Stork-Crabtree hydrogenation of **17** afforded the mono-hydrogenated product **40** also with a large *J* value in contrast to that of **19** from standard hydrogenations of **17**, indicating again a *trans* relationship between H6 and H7 in **40**. Aza-cycle **41**, prepared from *aza*-[4 + 2] cycloaddition of 1-azadiene and chiral allenamide **4**,[10a] is also suitable for this directed hydrogenation, giving the expected stereochemistry of the product. Given the unique conformational preference of **17**, **37**, and **41**, these studies unequivocally support a urea-directed Stork-Crabtree hydrogenation (see the box in Scheme 13).

(e) High Pressure Hydrogenations—The ultimate solution to this dilemma was using high-pressure hydrogenation. Even at 1500 *psi* of H_2, catalyst and solvent were still crucial to render this reaction feasible leading towards the desired pyran **26** rather than **20**. Using the best condition of 20% Pt-Alumina in hexanes for 3 d, **26** was isolated as a single isomer and in the acceptable yield of 50% and its stereochemistry was confirmed by using nOe (see the box in Scheme 14). From molecular modeling of **19** shown in Figure 2, both the urea group and TBDPS group do shield the bottom face of the pyran ring, thereby completely forcing H_2 to approach from the top face.

High-pressure hydrogenations of pyrans **28** and **40** were also examined. As shown in Scheme 15, an 89:11 isomeric ratio with respect to C3 stereochemistry was found of **44** while a 67:33 ratio was seen for **45**. At this point, we are not sure as to why in these two hydrogenations prefer the same face as the urea group.

It is noteworthy that collectively through these hydrogenation and epimerization studies, 6 of 8 possible diastereomers of pyran **26** could be attained from pyran **17** (Scheme 16).

5. Crotylation of Pyran 26 with *E*- and *Z*-Crotylsilane

With pyran **26** in hand, crotylation was then investigated. Promoted by $SnBr_4$, **26** was quickly epimerized to **44** with a large *J* constant meaning a *trans* relationship between H6 and H7. The following reaction with both *E*- and *Z*-crotylsilane proceeded smoothly and gave the crotylation products **50a** and **50b** in opposing ratios (**50a**:**50b** = 4:1 with *E*-crotylsilane and 1:3 with *Z*-crotylsilane), and the TBDPS group was also lost in the process. We believe that along with removal of the chiral imidazolidinone, the likely oxocarbenium ion intermediate **49** was generated in which the bulky alkyl group at C3 predominates and assumes an equatorial position.[10c,17] Then, addition of *E*- or *Z*-crotylsilane to **49** would prefer an anomerically axial trajectory, which is both stereoelectronically and sterically favorable, and provide the expected stereochemical outcome at C7. Based on this analysis, it turned out that **50a** and **50b** should be diastereomers at C8. Successive oxidation of **50a**/**50b** (as a 4:1 mixture) led to carboxylic acids **51a** and **51b**, which could be separated. The X-ray structure of **51a** unambiguously confirmed all relative stereochemistry. The assignment of C8 in **51a** suggests that **51b** would be the desired crotylation product for the synthesis.

The rationale for the stereochemical outcome at C8 can be illustrated employing Danishefsky's C3-crotylation model as shown in Scheme 18.[4k] In our C7-crotylations, when ruling out transition states from either the anti-periplanar or the synclinal approach with two excessive to severe gauche interactions, and when assuming an anomerically favored axial addition of *E*- or *Z*-crotylsilane, what is left behind would be a synclinal approach for the *E*-crotylation in which E^{S1} is more favored in leading to **50a**, whereas both anti-periplanar and synclinal

pathways could be at play for the *Z*-crotylation with Z^{A1} playing a more dominant role to favor the formation of **50b**.

6. Synthesis of the C1–C9 Subunit: Intercepting Cossy's Intermediate

To complete our synthesis of C1–C9 subunit, the crotylated pyran **50b** was carried on as a 3:1 isomeric mixture in a sequence of Dess-Martin periodinate oxidation and further oxidation, leading to carboxylic acid **51b** still as a 3:1 mixture (Scheme 19). Then, methylation and dihydroxylation of the formed methyl ester furnished the diol mixture **52**, in which the major isomer at C8 was readily separated as a 8:1 mixture at C9. Finally, oxidative cleavage of **53** with $Pb(OAc)_4$ provided aldehyde **6**, which spectroscopically matched Cossy's advanced intermediate. [4n]

CONCLUSION

We have described here a synthesis of the C1–C9 subunit of (+)-zincophorin that matches Cossy's advanced intermediate, thereby constituting a formal total synthesis, and details of an unusual urea-directed Stork-Crabtree hydrogenation of the hetero-[4 + 2] cycloadduct derived from a chiral allenamide. This work provides the first application of chiral allenamides in natural product synthesis.

EXPERIMENTAL SECTION

Preparation of pyran 17

To a solution of chiral enone **16** (2.48 g, 7.03 mmol) in anhyd CH_3CN (50 mL) was added allenamide **9** (2.22 g, 9.72 mmol). This reaction mixture was sealed under N_2 and heated up to 90 °C for 2 d. Concentration under reduced pressure and purification of the crude residue via silica gel flash column chromatography (gradient eluent: 10–20% EtOAc in hexanes) afforded pure cycloadduct **17** (1.96 g, 58% based on recovery of 17% **16**) of as a colorless oil. **17**: R_f = 0.50 [33% EtOAc/hexanes]; $[\alpha]_D^{25} = -100.4°$ [*c* 1.00, CH_2Cl_2]; ^{1}H NMR (500 MHz, $CDCl_3$) δ 0.59 (d, 3H, *J* = 6.5 Hz), 1.11 (d, 3H, *J* = 6.5 Hz), 1.13 (s, 9H), 2.23 (dd, 1H, *J* = 2.5, 20.5 Hz), 2.39 (m, 1H), 2.51 (dd, 1H, *J* = 4.0, 20.0 Hz), 2.71 (s, 3H), 3.56–3.63 (m, 2H), 3.84 (dd, 1H, *J* = 6.5, 10.0 Hz), 4.52 (dd, 1H, *J* = 3.6, 4.0 Hz), 4.78 (s, 1H), 4.86 (d, 1H, *J* = 8.5 Hz), 5.03 (s, 1H), 6.26 (s, 1H), 7.09–7.10 (m, 2H), 7.24–7.28 (m, 3H), 7.42–7.52 (m, 6H), 7.71–7.74 (m, 4H); ^{13}C NMR (125 MHz, $CDCl_3$) δ 14.7, 14.8, 19.3, 26.9, 26.8, 28.6, 41.3, 56.7, 59.5, 66.5, 80.9, 94.4, 114.7, 127.59, 127.63, 127.68, 127.7, 129.50, 129.57, 133.8, 134.2, 135.46, 135.54, 135.59, 137.78, 137.98, 154.3, 161.4; IR (neat) cm^{-1} 2957s, 1710s, 1456m, 1396s, 1361s; mass spectrum (APCI): m/e (% relative intensity) 581.2 (25) $(M+H)^+$, 439.3 (100), 405.2 (80), 279.2 (50), 191.2 (75), 101.1 (75); HRMS (MALDI) calcd for $C_{36}H_{45}N_2O_3Si$ $(M+H)^+$ 581.3199, found 581.3761.

Hydrogenation of pyran 17 to 19

To a heterogeneous mixture of Pt/C (5%w/w, 1.40 g, 0.33 mmol) and cycloadduct **17** (3.80 g, 6.55 mmol) in MeOH (140 mL) was added $NaBH_4$ (800.0 mg, 21.0 mmol) in small portions at 0 °C carefully over 2 min. The mixture was hydrogenated with a H_2-balloon for 2 h at rt, and after which, the catalyst was filtered and washed with MeOH (50 mL). The MeOH was removed under reduced pressure and the residue was diluted with Et_2O (100 mL). This mixture was washed with water (2 × 30 mL), dried over Na_2SO_4, and concentrated under reduced pressure. Purification of the crude residue via silica gel flash column chromatography (gradient eluent: 10–17% EtOAc in hexanes) afforded pure **19** (2.40 g, 64%) as a colorless oil. **19**: R_f = 0.50 [33% EtOAc/hexanes]; $[\alpha]_D^{25} = -29.9°$ [*c* 1.45, CH_2Cl_2]; ^{1}H NMR (500 MHz, $CDCl_3$) δ 0.67 (d, 3H, *J* = 6.5 Hz), 0.76 (d, 3H, *J* = 6.5 Hz), 1.14–1.16 (m, 12H), 1.22 (m, 1H), 1.94–2.04 (m, 2H), 2.43 (m, 1H), 2.75 (s, 3H), 3.63 (dd, 1H, *J* = 7.0, 9.5 Hz), 3.73 (dq, 1H, *J*

= 6.5 Hz), 3.88 (dd, 1H, *J* = 6.5, 10.0 Hz), 4.49 (dd, 1H, *J* = 3.5, 4.0 Hz), 4.78 (s, 1H, *J* = 8.5 Hz), 5.83 (d, 1 H, *J* = 3.5 Hz), 7.33 (m, 4H), 7.43–7.52 (m, 7H), 7.75–7.76 (m, 4H); ^{13}C NMR (125 MHz, $CDCl_3$) δ 14.9, 15.4, 15.6, 19.7, 27.2, 27.3, 29.0, 30.1, 41.5, 57.9, 58.8, 66.9, 83.0, 94.9, 127.89, 127.91, 127.93, 127.98, 129.84, 129.88, 134.26, 134.44, 135.87, 135.93, 139.22, 154.8, 163.5; IR (neat) cm^{-1} 2960s, 1710s, 1426s, 1393s, 1363m; mass spectrum (APCI): m/e (% relative intensity) 583.0 (20) $(M+H)^+$, 439.4 (100), 393.3 (50), 279.2 (30), 191.2 (20), 101.1 (75); HRMS (MALDI) calcd for $C_{36}H_{46}N_2O_3SiNa$ $(M+Na)^+$ 605.3170, found 605.3202.

Hydrogenation of pyran 19 to 26

A heterogeneous mixture of Pt/Alumina (5%w/w, 80.0 mg, 0.020 mmol) and **19** (60.0 mg, 0.10 mmol) in hexanes (5 mL) was hydrogenated under 1500 *psi* in a high-pressure bomb at rt for 3 d. After which, the catalyst was filtered and washed with EtOAc (10 mL). Concentration under reduced pressure and purification of the crude residue via silica gel flash column chromatography (gradient eluent: 10–17% EtOAc in hexanes) afforded pure **26** (31.0 mg, 50%) as a colorless oil. **26**: R_f = 0.50 [33% EtOAc/hexanes]; $[\alpha]_D^{25}$ = + 49.8 ° [*c* 1.00, CH_2Cl_2]; ^{1}H NMR (500 MHz, $CDCl_3$) δ 0.62 (d, 3H, *J* = 6.5 Hz), 0.69 (d, 3H, *J* = 6.5 Hz), 0.96 (d, 3H, *J* = 7.0 Hz), 1.11 (s, 9H), 1.20–1.30 (m, 2H), 1.49 (ddd, 1H, *J* = 2.0, 6.0, 13.0 Hz), 1.71–1.80 (m, 2H), 1.93 (m, 1H), 2.70 (s, 3H), 3.50–3.60 (m, 3H), 3.75 (dd, 1H, *J* = 5.5, 10.0 Hz), 4.65 (d, 1H, *J* = 8.5 Hz), 5.15 (d, 1H, *J* = 2.0 Hz), 7.26–7.30 (m, 4 H), 7.42–7.48 (m, 7H), 7.26–7.30 (m, 4H); ^{13}C NMR (125 MHz, $CDCl_3$) δ 12.6, 13.1, 15.5, 19.6, 22.3, 27.2, 28.9, 31.5, 31.6, 41.3, 57.8, 58.8, 66.1, 80.1, 86.5, 127.5, 127.8, 127.9, 129.8, 134.40, 134.44, 135.94, 135.95, 135.96, 136.00, 139.8, 168.2; IR (neat) cm^{-1} 2962s, 1708s, 1472m, 1427s, 1390s; mass spectrum (APCI): m/e (% relative intensity) 585.2 (100) $(M+H)^+$, 507.3 (30), 431.4 (20), 329.3 (80), 191.2 (30), 101.1 (90); HRMS (MALDI) calcd for $C_{36}H_{48}N_2O_3SiNa$ $(M+Na)^+$ 607.3332, found 607.3300.

Crotylation of pyran 26 to 50a/50b

To a solution of **26** (340.0 mg, 0.58 mmol) and *Z*-crotylsilane (270.0 μL, 1.74 mmol) in CH_2Cl_2 (30 mL) was added $SnBr_4$ (1.13 g, 2.32 mmol) at −78 °C. The reaction was warmed to −35 °C slowly and stirred at this temperature for 24 h with exposure to the air. Then the mixture was quenched by adding sat aq $NaHCO_3$ (10 mL), and extracted with CH_2Cl_2 (3 × 50 mL). The combined organic phases were washed with sat aq NaCl (2 × 15 mL), dried over Na_2SO_4, and concentrated under reduced pressure. Purification of the crude residue via silica gel flash column chromatography (gradient eluent: 7–14% EtOAc in hexanes) afforded a mixture of **50a** and **50b** (1:3, 80.0 mg, 65%) as a colorless oil. **50b**: R_f = 0.30 [20% EtOAc/hexanes]; ^{1}H NMR (500 MHz, $CDCl_3$) δ 0.84 (d, 3H, *J* = 7.0 Hz), 1.04 (d, 3H, *J* = 7.0 Hz), 1.06 (d, 3H, *J* = 7.0 Hz), 1.35–1.40 (m, 1H), 1.48–1.63 (m, 2H), 1.70–1.88 (m, 3H), 2.71 (m, 1H), 3.19 (dd, 1H, *J* = 3.0, 9.0 Hz), 3.41 (bs, 1H), 3.47 (ddd, 1H, *J* = 3.5, 9.0, 9.0 Hz), 3.60 (m, 1 H), 5.00 (d, 1H, *J* = 10.5 Hz), 5.05 (d, 1H, *J* = 16.5 Hz), 5.64 (ddd, 1H, *J* = 8.0, 10.0, 17.0 Hz); ^{13}C NMR (100 MHz, $CDCl_3$) δ 13.9, 16.1, 18.6, 24.9, 25.0, 28.4, 38.3, 39.1, 68.2, 76.5, 81.9, 114.9, 142.1. **50a**: ^{1}H NMR (500 MHz, $CDCl_3$) δ 0.80 (d, 3H, *J* = 6.5 Hz), 0.99 (d, 3H, *J* = 7.0 Hz), 1.03 (d, 3H, *J* = 7.0 Hz), 1.36–1.41 (m, 1H), 1.50–1.60 (m, 2H), 1.69–1.78 (m, 2H), 1.81–1.87 (m, 1H), 2.65 (m, 1H), 3.06 (dd, 1H, *J* = 4.0, 8.0 Hz), 3.21 (dd, 1H, *J* = 4.0, 8.0 Hz), 3.48–3.55 (m, 1H), 3.57 (dd, 1 H, *J* = 4.0, 10.6 Hz), 3.57–3.64 (m, 1H), 5.05 (d, 1H, *J* = 10.0 Hz), 5.07 (d, 1H, *J* = 15.0 Hz), 5.84 (ddd, 1H, *J* = 8.5, 10.0, 15.0 Hz); ^{13}C NMR (100 MHz, $CDCl_3$) δ 18.47, 18.50, 25.2, 25.7, 29.1, 38.0, 38.9, 67.7, 76.1, 81.7, 114.6, 141.4; IR (neat) cm^{-1} 3439s, 2961s, 1640w, 1459s, 1376m; mass spectrum (APCI): m/e (% relative intensity) 213.3 (100) $(M+H)^+$, 195.2 (85), 177.2 (90), 157.2 (30), 139.2 (45); HRMS (ESI) calcd for $C_{13}H_{24}O_2Na$ $(M+Na)^+$ 235.1674, found 235.1673.

Supplementary Material

Refer to Web version on PubMed Central for supplementary material.

ACKNOWLEDGEMENT

The authors thank the NIH [GM066055] for funding and Mr. Benjamin E. Kucera and Dr. Vic Young from University of Minnesota for providing X-ray structural analysis.

REFERENCES

1. Westley, JW., editor. Polyether Antibiotics. Vol. 1. New York: Marcel Dekker; 1982. Vol. 2. 1983Dobler, M., editor. Ionophores and their Structures. New York: Wiley; 1981.
2. For isolation, see: Grafe U, Schade W, Roth M, Radics L, Incze M, Ujszaszy K. J. Antibiot 1984;37:836–846. [PubMed: 6434502] (b) Brooks HA, Gardner D, Poyser JP, King TJ. J. Antibiot 1984 37;:1501–1504. [PubMed: 6549004] (c) Radics L. J. Chem. Soc., Chem. Commun 1984:599–601.Gräfe, U. German. [East]: DD 231,793
3. Tonew E, Tonew M, Gräfe U, Zopel P. Pharmazie 1988;43:717–719. [PubMed: 3212020]
4. For approaches, see: (a) Cossy J, Blanchard N, Defosseux M, Meyer C. Angew. Chem., Int. Ed 2002;41:2144–2146. (b) Guindon Y, Murtagh L, Caron V, Landry SR, Jung G, Bencheqroun M, Faucher A-M, Guerin B. J. Org. Chem 2001;66:5427–5437. [PubMed: 11485466] (c) Burke SD, Ng RA, Morrison JA, Alberti MJ. J. Org. Chem 1998;63:3160–3161. (d) Marshall JA, Palovich MR. J. Org. Chem 1998;63:3701–3705. (e) Chemler SR, Roush WR. J. Org. Chem 1998;63:3800–3801. (f) Booysen JF, Holzapfel CW. Synth. Commun 1995;25:1473–1488. (g) Cywin CL, Kallmerten J. Tetrahedron Lett 1993;34:1103–1106. (h) Balestra M, Wittman MD, Kallmerten J. Tetrahedron Lett 1988;29:6905–6908. (i) Zelle RE, DeNinno MP, Selnick HG, Danishefsky SJ. J. Org. Chem 1986;51:5032–5036. The first total synthesis, see: (j) Danishefsky SJ, Selnick HG, DeNinno MP, Zelle RE. J. Am. Chem. Soc 1987;109:1572–1574. (k) Danishefsky SJ, Selnick HG, Zelle RE, DeNinno MP. J. Am. Chem. Soc 1988;110:4368–4378. For Cossy's total synthesis, see: (l) Cossy J, Meyer C, Defosseux M, Blanchard N. Pure Appl. Chem 2005;77:1131–1137. (m) Defosseux M, Blanchard N, Meyer C, Cossy J. J. Org. Chem 2004;69:4626–4647. [PubMed: 15230584] (n) Defosseux M, Blanchard N, Meyer C, Cossy J. Org. Lett 2003;5:4037–4040. [PubMed: 14572243] For Miyashita's total synthesis, see: (o) Komatsu K, Tanino K, Miyashita M. Angew. Chem. Int. Ed 2004;43:4341–4345.
5. Song Z, Hsung PR. Org. Lett 2007;9:2199–2202. [PubMed: 17480091]
6. Wei L-L, Hsung RP, Xiong H, Mulder JA, Nkansah NT. Org. Lett 1999;1:2145–2148.
7. For reviews on allenamides, see: (a) Hsung RP, Wei L-L, Xiong H. Acc. Chem. Res 2003;36:773–782. [PubMed: 14567711] (b) TraceyMRHsungRPAntolineJKurtzKCMShenLSlaferBWZhangYSteveMWeinrebChapter 21.4. Science of Synthesis, Houben-Weyl Methods of Molecular Transformations2005Stuttagart, GermanyGeorg Thieme Verlag KG
8. For recent reports on the allenamide chemistry, see: (a) Parthasarathy K, Jeganmohan M, Cheng C-H. Org. Lett 2006;8:621–623. [PubMed: 16468726] (b) Fenández I, Monterde MI, Plumet J. Tetrahedron Lett 2005;46:6029–6031. (c) de los Rios C, Hegedus LS. J. Org. Chem 2005;70:6541–6543. [PubMed: 16050728] (d) Alouane N, Bernaud F, Marrot J, Vrancken E, Mangeney P. Org. Lett 2005;7:5797–5800. [PubMed: 16354069] (e) Antoline JE, Hsung RP, Huang J, Song Z, Li G. Org. Lett 2007;9:1275–1278. [PubMed: 17335226] (f) Huang J, Ianni JC, Antoline JE, Hsung RP, Kozlowski MC. Org. Lett 2006;8:1565–1568. [PubMed: 16597111] (g) Berry CR, Hsung RP, Antoline JE, Petersen ME, Rameshkumar C, Nielson JA. J. Org. Chem 2005;70:4038–4042. [PubMed: 15876094] (h) Shen L, Hsung RP, Zhang Y, Antoline JE, Zhang X. Org. Lett 2005;7:3081–3084. [PubMed: 15987210] (i) Huang J, Hsung RP. J. Am. Chem. Soc 2005;127:50–51. [PubMed: 15631443]
9. For some recent elegant studies on related inverse demand hetero [4 + 2] cycloaddition of chiral enamides, see: (a) Gohier F, Bouhadjera K, Faye D, Gaulon C, Maisonneuve V, Dujardin G, Dhal R. Org. Lett 2007;9:211–214. [PubMed: 17217267] (b) Tardy S, Tatibouët A, Rollin P, Dujardin G. Synlett 2006:1425–1427. and reference cited therein. Also see: (c) Palasz A. Org. Biomol. Chem 2005;3:3207–3212. [PubMed: 16106303]

10. (a) Berry CR, Hsung RP. Tetrahedron 2004;60:7629–7636. (b) Wei L-L, Xiong H, Douglas CJ, Hsung RP. Tetrahedron Lett 1999;40:6903–6907. (c) Berry CR, Rameshkumar C, Tracey MR, Wei L-L, Hsung RP. Synlett 2003:791–796. (d) Rameshkumar C, Hsung RP. Synlett 2003:1241–1246.
11. Close WJ. J. Org. Chem 1950;15:1131–1134.
12. (a) Fuerstner A, Kattnig E, Lepage O. J. Am. Chem. Soc 2006;128:9194–9204. [PubMed: 16834393] (b) Bergmeier SC, Stanchina DM. J. Org. Chem 1997;62:4449–4456. [PubMed: 11671773]
13. (a) Crabtree RH, Davis MW. J. Org. Chem 1986;51:2655–2661. (b) Crabtree RH. Acc. Chem. Res 1979;12:331–337.
14. For the first application of directed hydrogenations employing Crabtree's catalyst, see: (a) Stork G, Kahne DE. J. Am. Chem. Soc 1983;105:1072–1073. For some leading applications, also see: (b) Evans DA, Morrissey MM. J. Am. Chem. Soc 1984;106:3866–3868. (c) Ginn JD, Padwa A. Org. Lett 2002;4:1515–1517. [PubMed: 11975617]
15. For an amide directed hydroboration using Crabtree's catalyst, see: (a) Evans DA, Fu GC. J. Am. Chem. Soc 1991;113:4042–4043. (b) Evans DA, Fu GC, Hoveyda AH. J. Am. Chem. Soc 1992;114:6671–6679.
16. For a review on directed reactions, see: (a) Hoveyda AH, Evans DA, Fu GC. Chem. Rev 1993;93:1307–1370. For a highlight related to Crabtree's catalyst, see: (b) Nell PG. Synlett 2001:160.
17. Romero JAC, Tabacco SA, Woerpel KA. J. Am. Chem. Soc 2000;122:168–169.

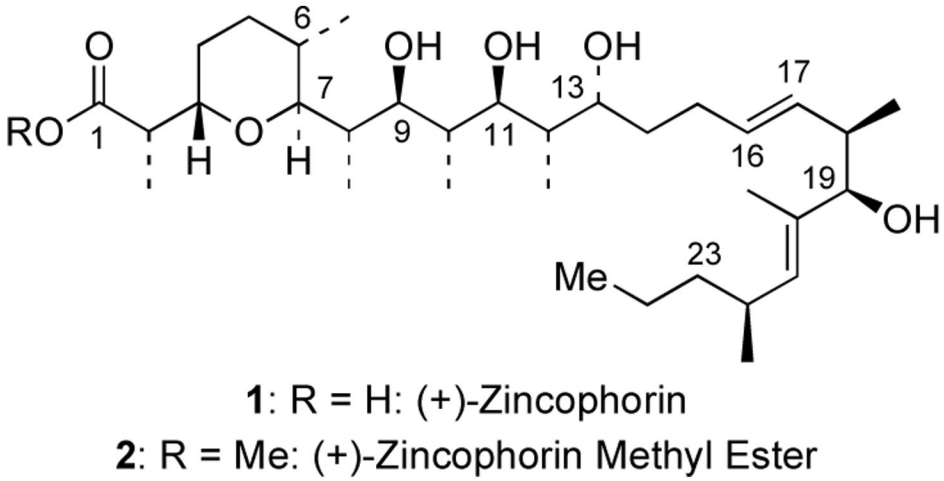

1: R = H: (+)-Zincophorin

2: R = Me: (+)-Zincophorin Methyl Ester

Figure 1.
(+)-Zincophorin and Its Methyl Ester.

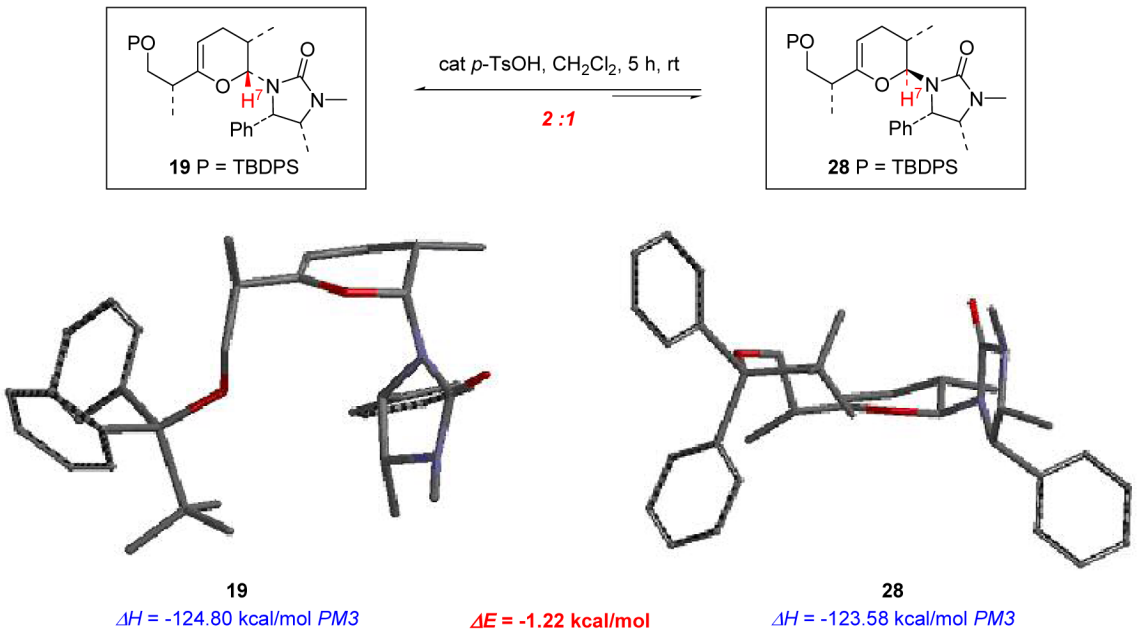

Figure 2.
Molecular Modeling of Pyran **19** and **28**.

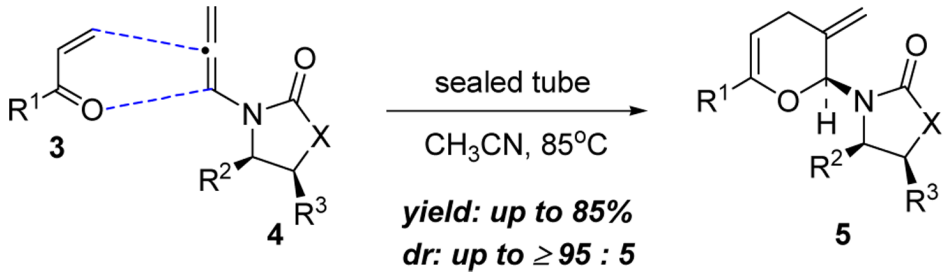

Scheme 1.
An Inverse Electron Demand Hetero-[4 + 2] Cycloaddition.

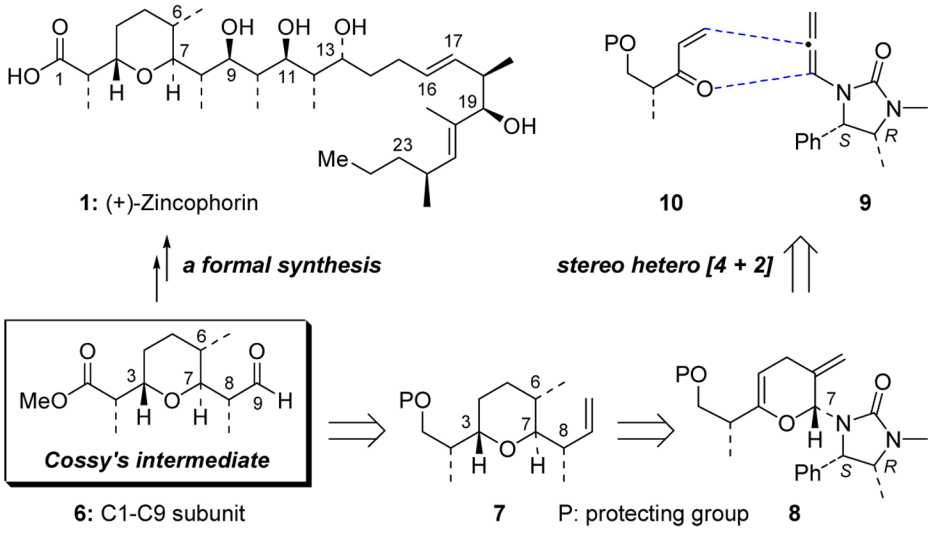

Scheme 2.
An Approach to C1–C9 Subunit of (+)-Zincophorin.

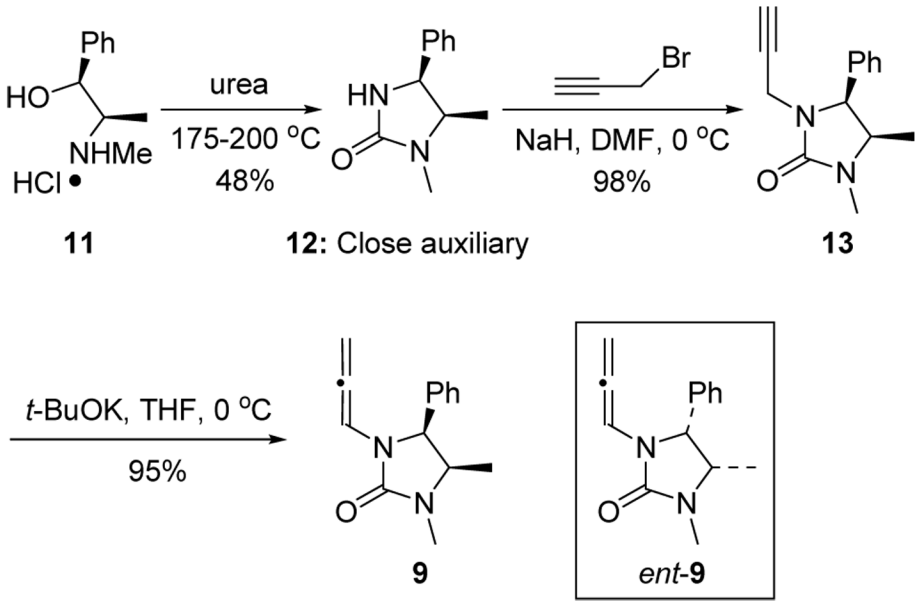

Scheme 3.
Synthesis of Chiral Allenamide **9**.

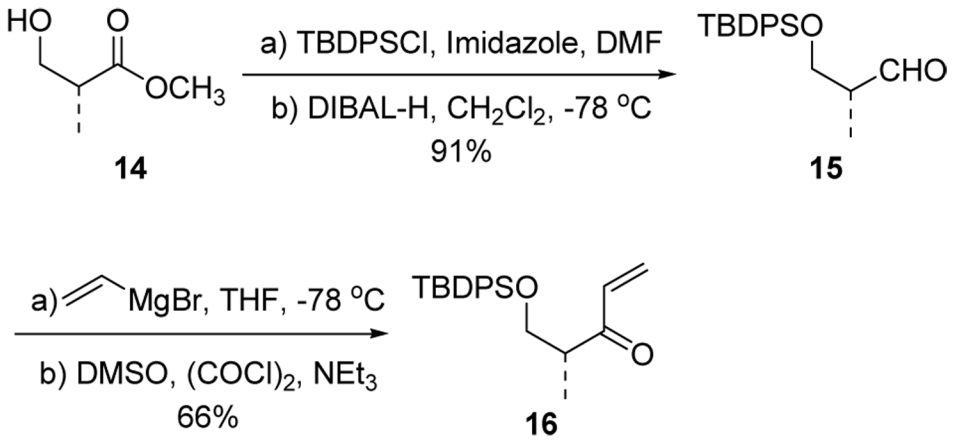

Scheme 4.
Synthesis of Chiral Enone **16**.

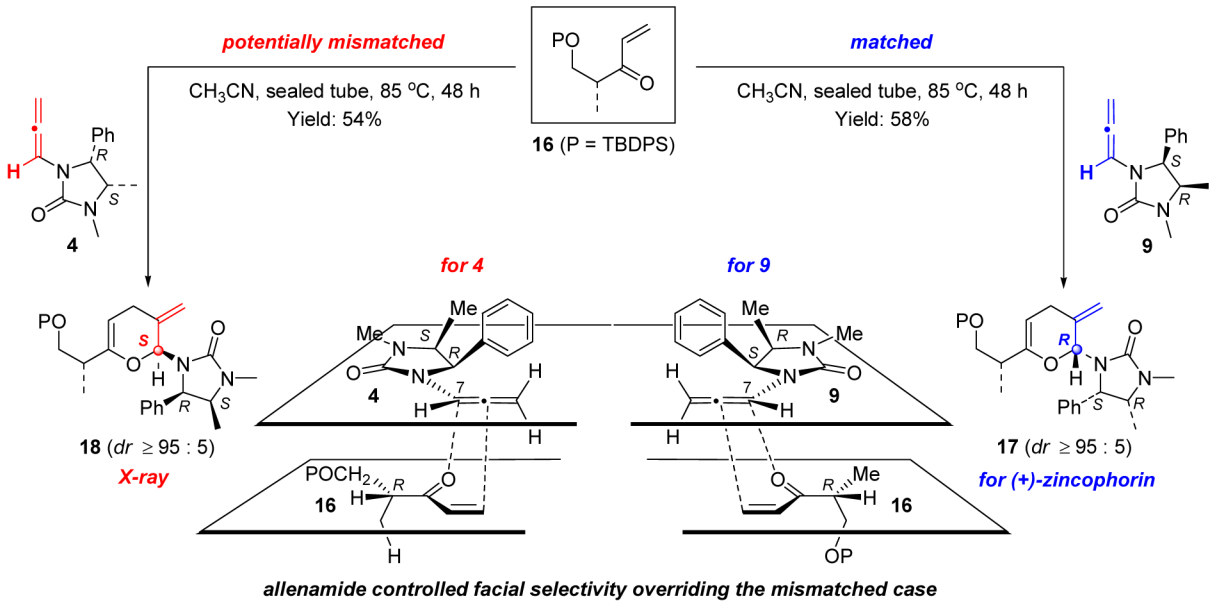

Scheme 5.
Hetero-[4 + 2] Cycloadditions with Chiral Enone **16**.

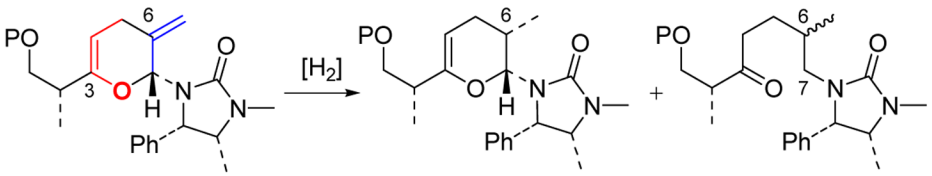

17 P = TBDPS **19** **20** (ratio ≅ 3:2)

entry	catalyst [mol%]	solvent	pressure	time [h]	yield [%]: **19**	**20**
1	Lindlar (5)	MeOH	1 atm	48	44	23
2	Lindlar (5)	MeOH	60 *psi*	3	30	30
3	Lindlar (5)	EtOAc	1 atm	24	20	45
4	Pd/C (5)	Hexanes (anhyd)	60 *psi*	24	22	44
5	Pt/C (5)	MeOH	1 atm	1	12	72
6	Pt/C (5)	MeOH	No H_2	0.5		NR
7	Pt/C (5) 30% Na_2CO_3	Hexanes (anhyd)	60 *psi*	1	47	39
8	**Pt/C (5) 3.0 equiv $NaBH_4$**	**MeOH**	**1 atm**	**2**	**64**	**12**

Scheme 6.
Hydrogenation of the C6 *Exo*-Cyclic Olefin in **17**.

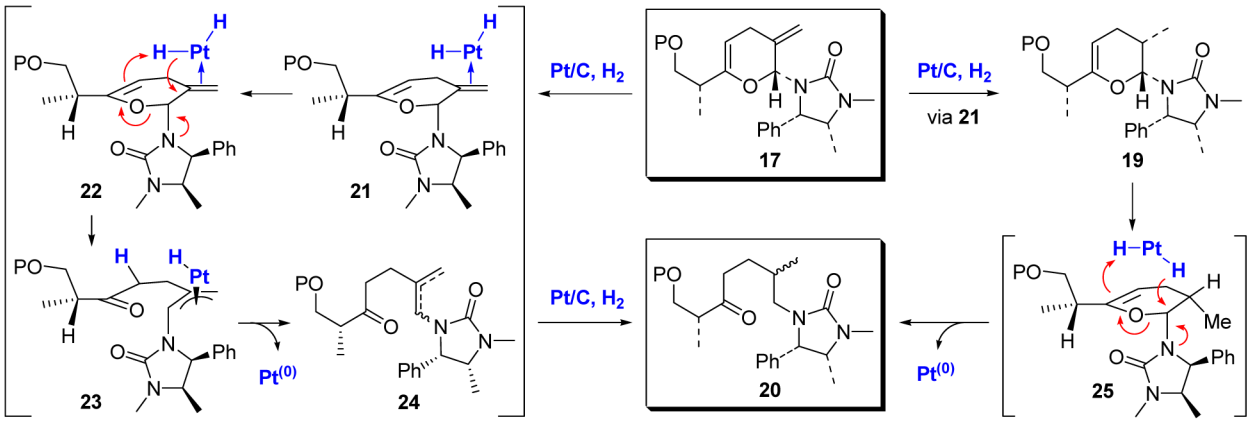

Scheme 7.
A Proposed Mechanism for the Formation of Ketone **20**.

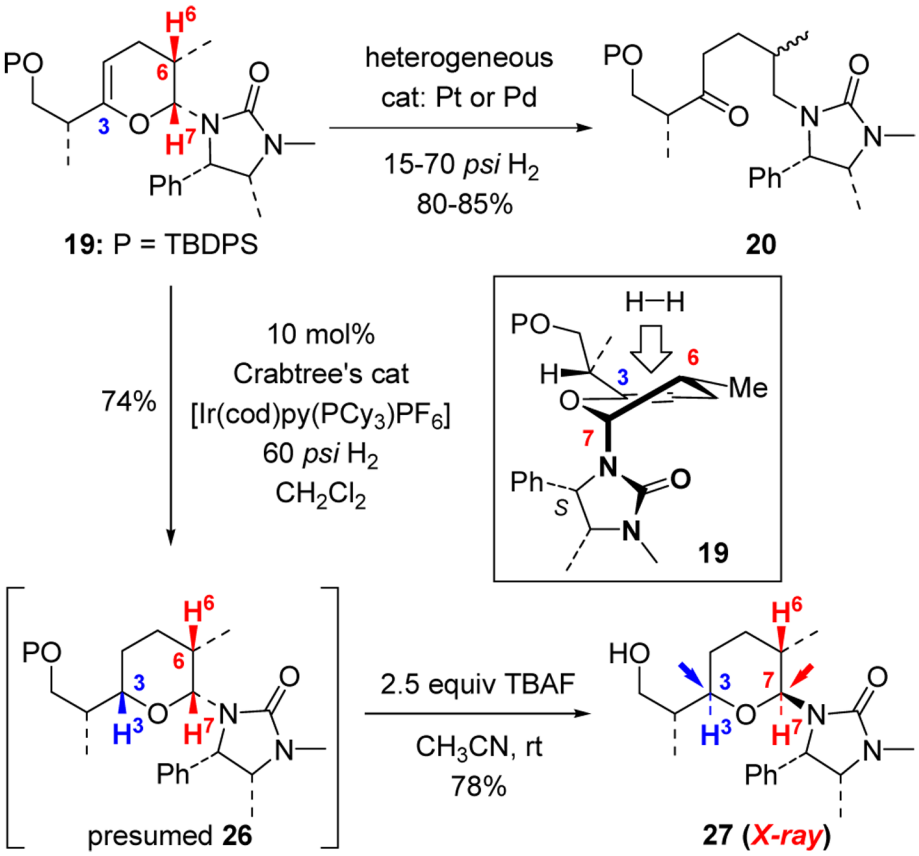

Scheme 8.
Hydrogenation of Pyran **19**.

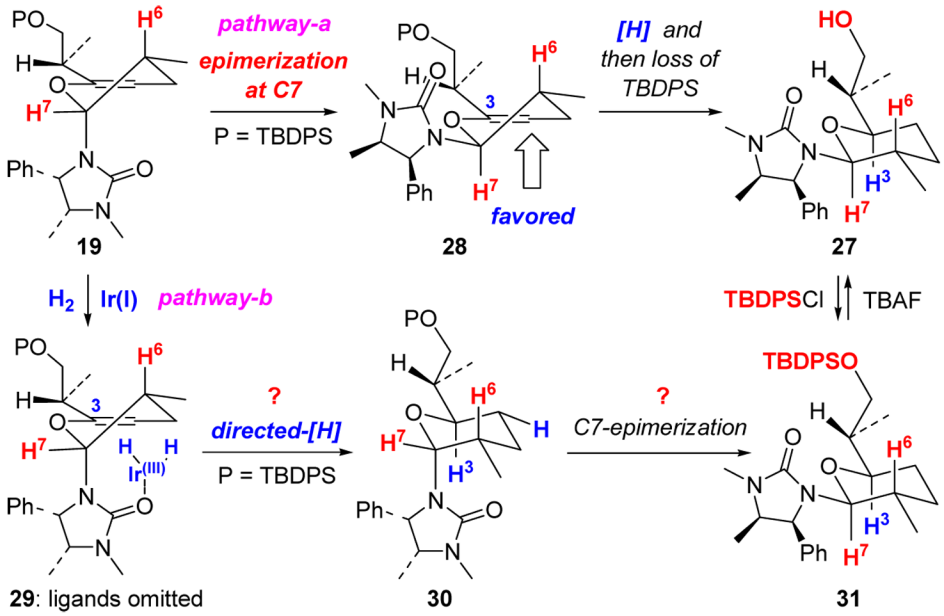

Scheme 9.
A Urea-Directed Hydrogenation vs Epimerization.

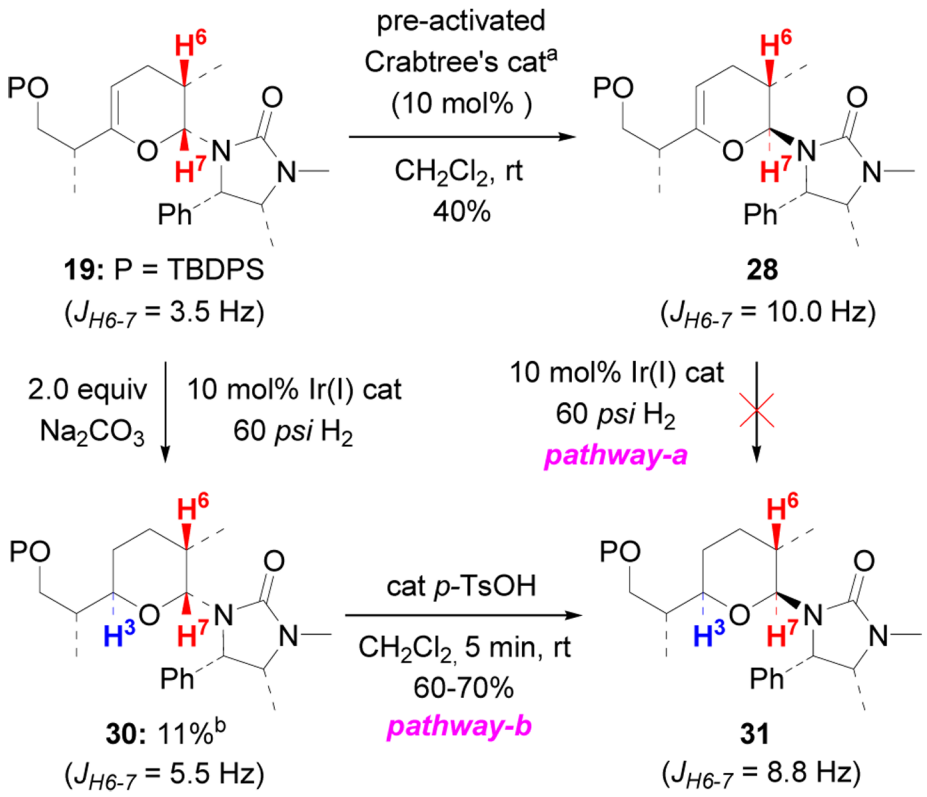

Scheme 10.

Experimental Support for **Pathway b**.

a. Crabtree's catalyst was pre-activated by treatment with 60 *psi* H_2 in CH_2Cl_2 at rt for 5 min.

b. 30 was obtained as an unseparated mixture with **19** (1:2); **31** was isolated in 35% yield.

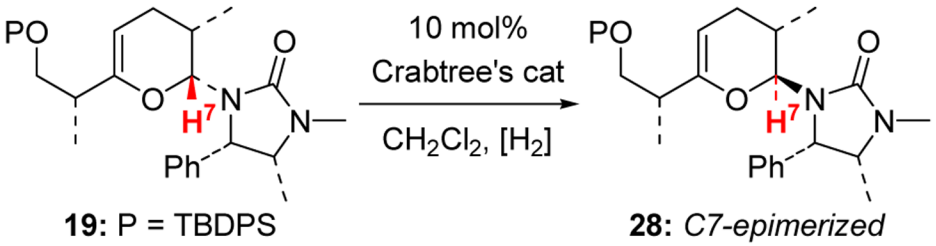

19: P = TBDPS

28: *C7-epimerized*

entry	pressure [*psi*]	**28**	**31**
1[a]	0	40%	0%
2	30	20%	0%
3	60	9%	74%

a: pre-activated catalyst was used.

\+

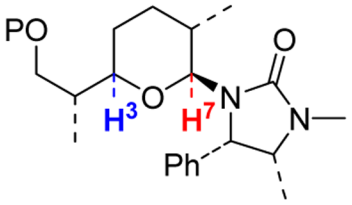

31: *Directed-[H]*

Scheme 11.
Directed Hydrogenation *versus* Epimerization.

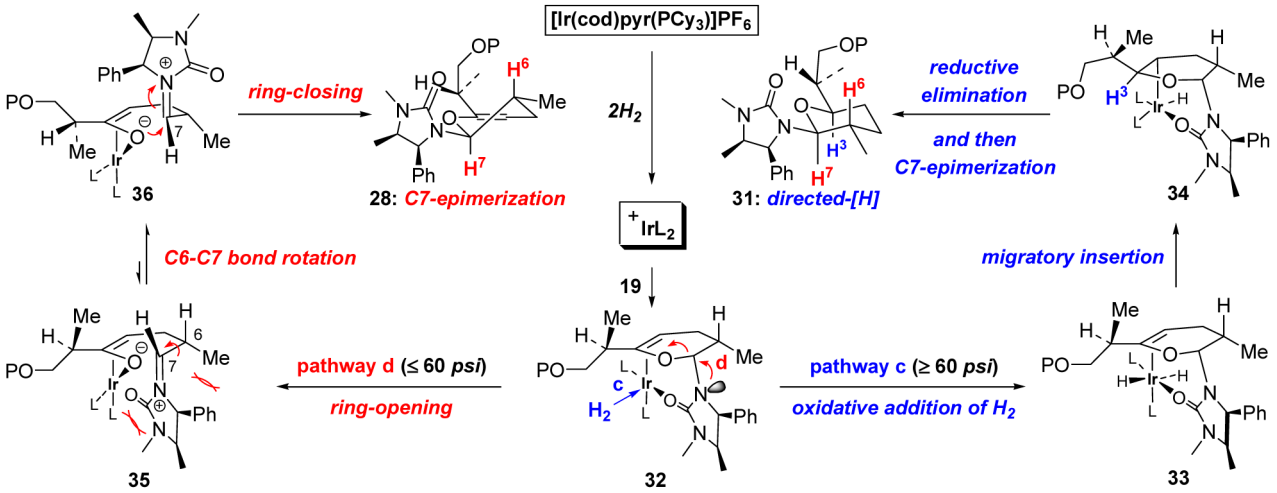

Scheme 12.
Competition Between Directed Hydrogenation and C7-Epimerization.

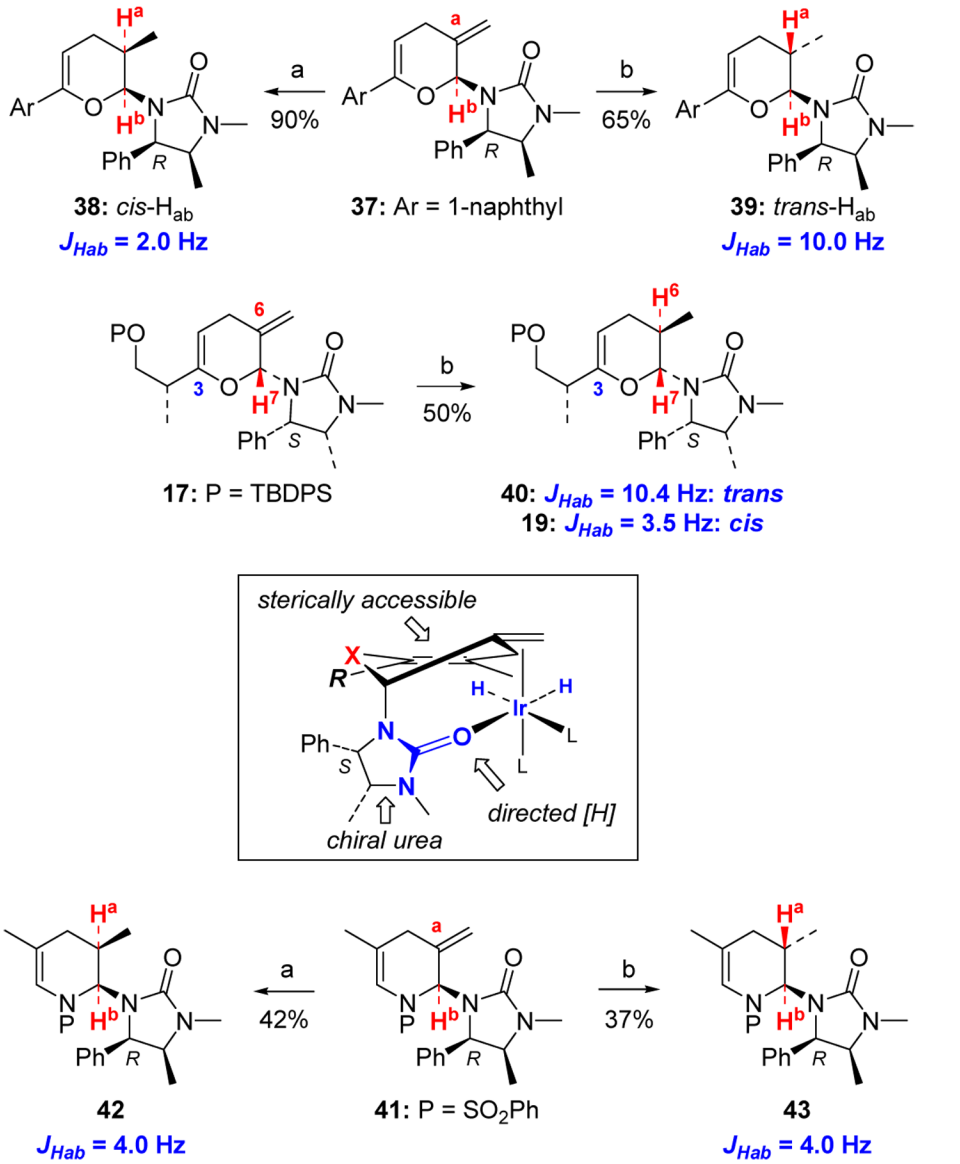

Scheme 13.

Scope of A Urea-Directed Stork-Crabtree Hydrogenation.

a: 5–10% Heterogeneous catalyst (Pd/C, Pt/C or Lindar), 1 atm H_2; **b:** 10 mol% Crabtree cat, 60 *psi* H_2, CH_2Cl_2.

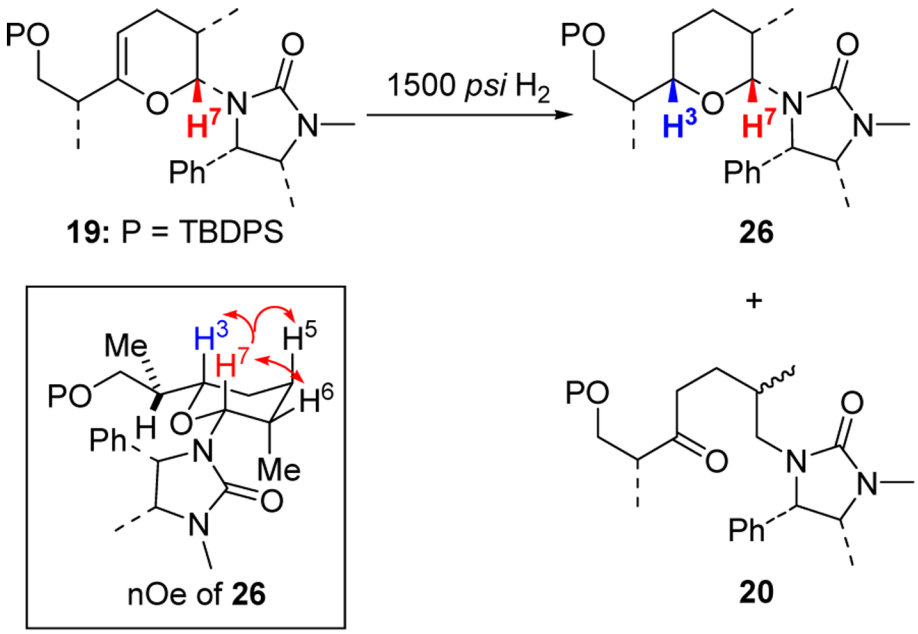

entry	catalyst [mol%]	solvent	time [h]	yield [%]: **26**	**20**
1	Lindlar (10)	MeOH	24 h	NR	
2	Pt/C (5)	MeOH	1 h	14	71
3	Pt/C (5)	EtOAc	1 h	14	64
4	Pt/C (5)	Hexanes	18 h	27	58
5	Pt/Alumina (20)	EtOAc	24 h	41	45
6	**Pt/Alumina (20)**	**Hexanes**	**3 d**	**50**	**25**

Scheme 14.
High-Pressure Hydrogenations of Pyran **19**.

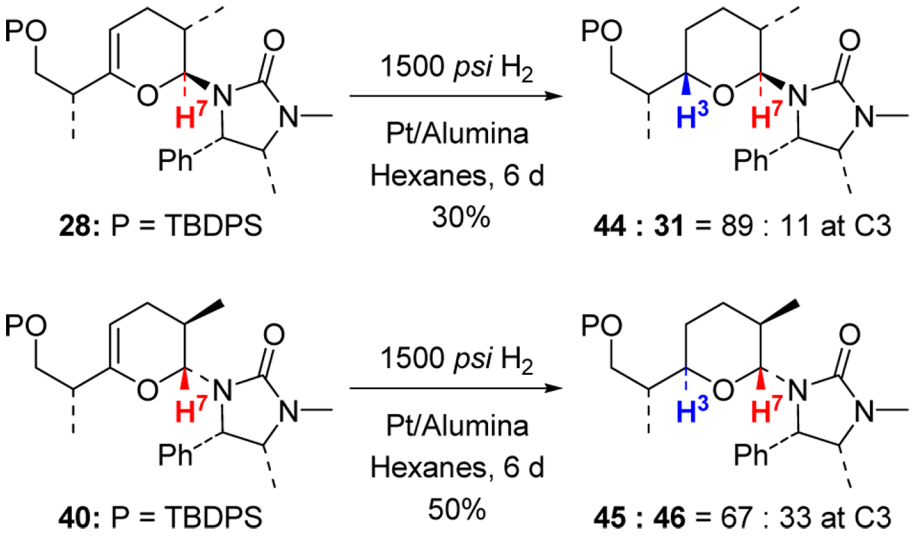

Scheme 15.
High-Pressure Hydrogenations of Pyrans **28** and **40**.

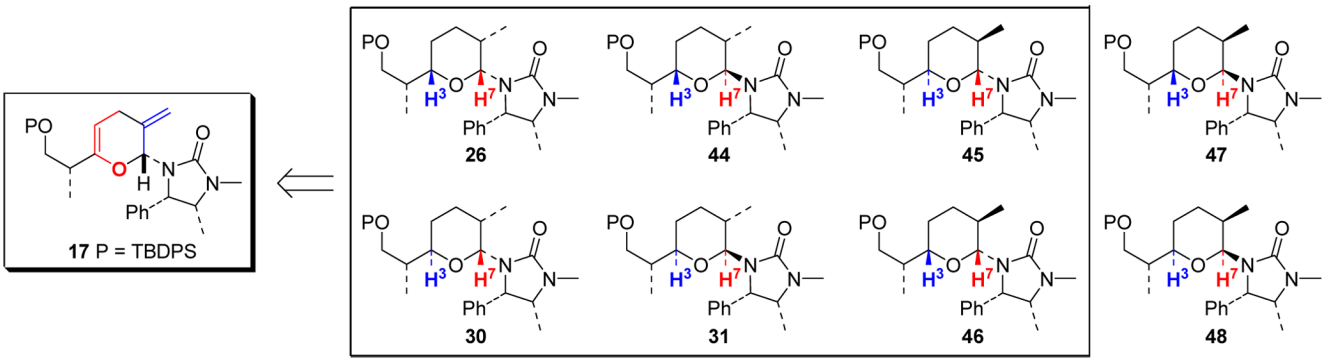

Scheme 16.

Summary: 6 Out of 8 Possible Diastereomers Attainable from Reduction of Pyran **17**.

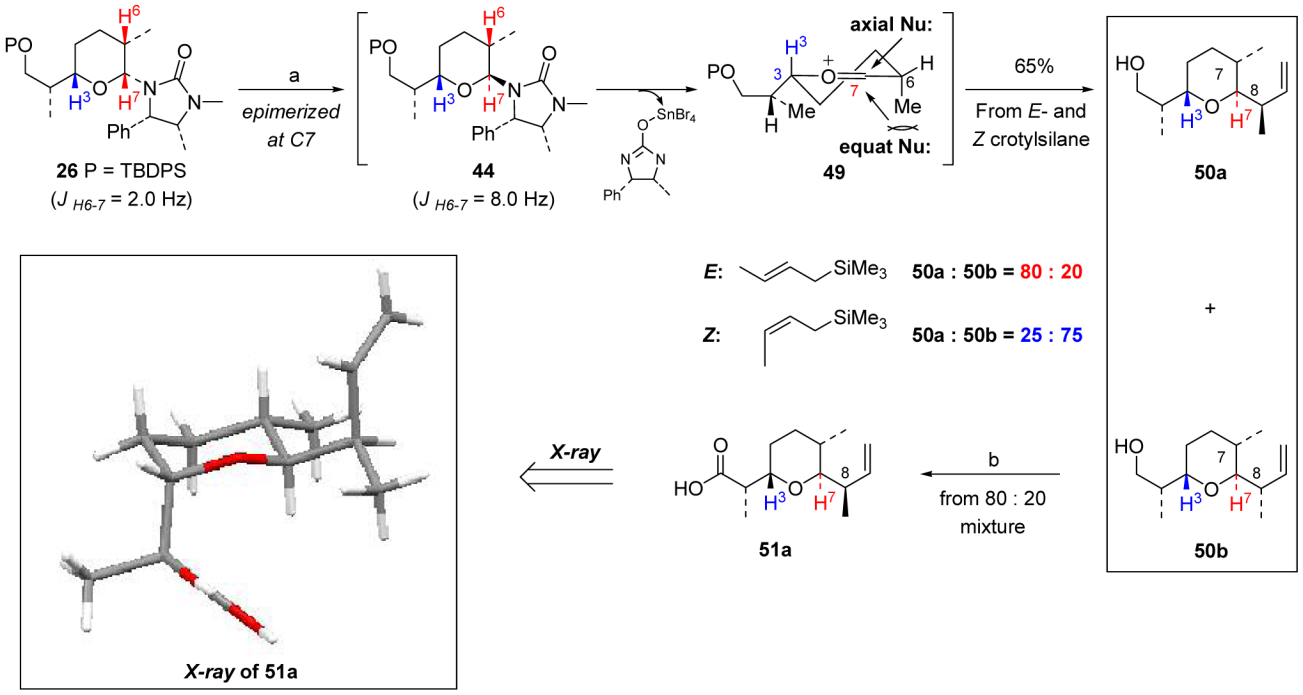

Scheme 17.

Crotylation of **26** with *E* and *Z*-Crotylsilane.

a: 4.0 equiv $SnBr_4$, CH_2Cl_2, −78 °C to - 35 °C, 24 h, 65%; **b:** 1) Dess-Martin [O], 96%; 2) NaH_2PO_4, $NaClO_2$, *t*-BuOH/H_2O, 2-Me-2-butene, 85%; 3) Separation of **51a** and **51b**.

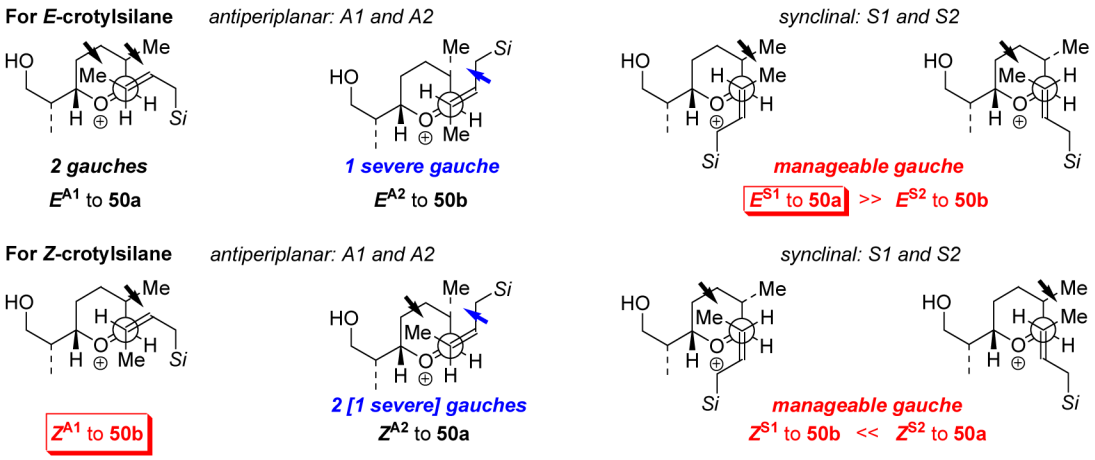

Scheme 18.
Rationale for the Stereochemical Outcome at C8.

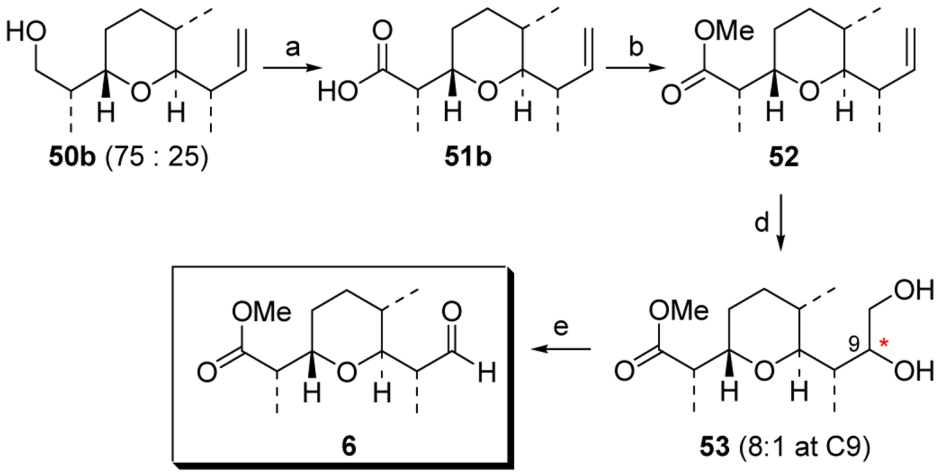

Scheme 19.

Intercepting Cossy's Intermmediate: C1–C9 Subunit.

a: 1. Dess-Martin [O], 98%; 2. NaH_2PO_4, $NaClO_2$,*t*-BuOH/H_2O, 2-Me-2-butene, 96%; **b:** $TMSCHN_2$, MeOH/toluene, 90%; **c:** NMO, OsO_4, acetone/H_2O, 79%; separation of the major isomer at C8 completely; **d:** $Pb(OAc)_4$, CH_2Cl_2, 53%.